Vincenza Cifarelli,[1] Laura M. Lashinger,[2] Kaylyn L. Devlin,[3] Sarah M. Dunlap,[2] Jennifer Huang,[2] Rudolf Kaaks,[4] Michael N. Pollak,[5] and Stephen D. Hursting[2,6,7]

Metformin and Rapamycin Reduce Pancreatic Cancer Growth in Obese Prediabetic Mice by Distinct MicroRNA-Regulated Mechanisms

Diabetes 2015;64:1632–1642 | DOI: 10.2337/db14-1132

OBESITY STUDIES

Metformin treatment is associated with a decreased risk and better prognosis of pancreatic cancer (PC) in patients with type 2 diabetes, but the mechanism of metformin's PC growth inhibition in the context of a prediabetic state is unknown. We used a Panc02 pancreatic tumor cell transplant model in diet-induced obese (DIO) C57BL/6 mice to compare the effects of metformin and the direct mammalian target of rapamycin (mTOR) inhibitor rapamycin on PC growth, glucose regulation, mTOR pathway signaling, and candidate microRNA (miR) expression. In DIO/prediabetic mice, metformin and rapamycin significantly reduced pancreatic tumor growth and mTOR-related signaling. The rapamycin effects centered on decreased mTOR-regulated growth and survival signaling, including increased expression of let-7b and cell cycle–regulating miRs. Metformin (but not rapamycin) reduced glucose and insulin levels and expression of miR-34a and its direct targets Notch, Slug, and Snail. Metformin also reduced the number and size of Panc02 tumor spheres in vitro and inhibited the expression of Notch in spheroids. Our results suggest that metformin and rapamycin can both inhibit pancreatic tumor growth in obese, prediabetic mice through shared and distinct mechanisms. Metformin and direct mTOR inhibitors, alone or possibly in combination, represent promising intervention strategies for breaking the diabetes-PC link.

Type 2 diabetes (T2D) is a progressive metabolic disorder affecting nearly 30 million Americans (~9.3% of the population) and is associated with obesity and increased risk of developing and dying from cancer (1). More specifically, the risk of developing pancreatic cancer (PC) is twice that of the nondiabetic population (2,3). Prediabetes, defined as having elevated fasting glucose and impaired glucose tolerance, is rising in prevalence even faster than T2D, with nearly 90 million prediabetic Americans (including 51% of Americans >65 years of age) (1). This is of particular concern regarding PC since >80% of PC cases develop after age 60 (2). Putative mechanistic explanations for the link between prediabetes, T2D, and PC include chronic hyperinsulinemia, oxidative stress, and inflammation (4).

Epidemiologic studies suggest that metformin, a widely used drug for the treatment of T2D (5), is associated with reduced risk among patients with diabetes of being either diagnosed with, or dying from, PC (6–8). However, whether these associations reflect a genuine protective action of metformin, as compared with other antidiabetic drugs, or whether they are the result of confounding (since T2D patients prescribed metformin may have very different clinical characteristics than T2D patients taking sulfonylurea or other glucose-lowering medications), remains unclear (9,10). Moreover, the

[1]Department of Medicine, Center for Human Nutrition, Washington University School of Medicine, St. Louis, MO
[2]Department of Nutritional Sciences, The University of Texas at Austin, Austin, TX
[3]Institute for Cellular and Molecular Biology, The University of Texas at Austin, Austin, TX
[4]Division of Epidemiology, German Cancer Research Center, Heidelberg, Germany
[5]Departments of Medicine and Oncology, McGill University, Montreal, Canada
[6]Department of Nutrition, University of North Carolina, Chapel Hill, NC
[7]Lineberger Comprehensive Cancer Center, University of North Carolina, Chapel Hill, NC

Corresponding author: Stephen D. Hursting, hursting@email.unc.edu.

Received 26 July 2014 and accepted 25 November 2014.

This article contains Supplementary Data online at http://diabetes.diabetesjournals.org/lookup/suppl/doi:10.2337/db14-1132/-/DC1.

V.C. and L.M.L. contributed equally to this work.

potential PC chemoprotective effects of metformin are not well understood.

Metformin can diminish hepatic glucose output, resulting in improved insulin sensitivity; it can also exert direct effects on tumor cell signaling (11,12). Direct cellular effects of metformin involve inhibition of ATP production, increased AMP kinase (AMPK) activity (13), and inhibition of the mammalian target of rapamycin (mTOR), a complex that couples protein synthesis to external growth factors and intracellular energy stores (14). Recent evidence indicates that this effect on mTOR is accomplished through transcription factor, Sp1-mediated downregulation of IGF-1 signaling (12). Inhibition of mTOR decreases cell proliferation in several cancer cell lines, including PC cells (12,15).

Rapamycin, a specific mTOR inhibitor, inhibits several processes involved in tumor cell proliferation and survival (16,17). Despite their shared mTOR inhibitory effects, rapamycin and metformin differentially influence other targets, including several microRNAs (miRs), noncoding RNA molecules that posttranscriptionally regulate gene expression (18). miRs regulate cellular processes involved in cancer initiation, recurrence, and metastasis (19).

To our knowledge, a direct comparison between the effects of metformin and rapamycin on PC outcomes in the context of diet-induced obesity (DIO) and prediabetes has not yet been reported. We chose to use a model of prediabetes characterized by hyperglycemia and insulin resistance since prediabetes is an established risk factor for PC (1), and people with prediabetes are becoming more prevalent in the U.S. and represent an important population for cancer prevention and treatment. The aim of this study was to compare metformin and rapamycin with respect to PC growth, systemic glucose metabolism, mTOR pathway signaling, candidate miR expression, and cancer stem cell (CSC) and epithelial-to-mesenchymal transition (EMT) characteristics using a syngeneic murine PC transplant model in DIO/prediabetic mice.

RESEARCH DESIGN AND METHODS

Mice, Diet, and Experimental Design

Mice were singly housed in a semibarrier facility in the Animal Resource Center at The University of Texas; the Institutional Animal Care and Use Committee approved all experimentation.

Seventy-five male 6-week-old C57BL/6 mice (The Jackson Laboratory, Bar Harbor, ME) were administered a DIO diet (D12492; Research Diets) throughout the study. After 15 weeks of DIO, mice were randomized (25 per group) to receive either *1*) metformin (250 mg/kg continuously in drinking water), *2*) rapamycin (2.5 mg/kg, administered i.p. every other day; LC Laboratories, Woburn, MA), or *3*) vehicle control (0.1% DMSO, in 0.9% saline, i.p. every other day) for 5 weeks. The metformin group received vehicle injections every other day, whereas the rapamycin and vehicle control groups were provided ad libitum access to drinking water without metformin. The rapamycin dose of 2.5 mg/kg was chosen to achieve inhibition of phosphorylation of mTOR based on our previous studies (20). At week 19 on study (4 weeks of drug treatment), 10 mice per group underwent glucose tolerance test and insulin tolerance test (as previously described [20,21]) and then were killed and their tissues collected and stored. At 20 weeks on study, the remaining mice (n = 15 per group) were injected (subcutaneously) in the right flank with 5×10^5 Panc02 murine PC cells (maintained in McCoy's media as previously described [22]) and continued on their diet regimen for an additional 4 weeks while tumor growth was monitored. Food intake and body weights were recorded weekly. At study termination (week 24), all mice were fasted for 6 h and anesthetized by CO_2 inhalation and then blood was collected via cardiac puncture. Blood samples were centrifuged at 9,300*g* for 5 min and serum collected and stored at −80°C. Pancreatic tumors were either snap frozen in liquid nitrogen and stored at −80°C or fixed with 10% neutral-buffered formalin overnight, paraffin embedded, and used for histologic and immunohistochemical analyses as described below.

Serum Hormones and Adipokines

Serum insulin, IGF-1, resistin, and adiponectin concentrations were measured in mice (vehicle, n = 11; metformin, n = 14; rapamycin, n = 14) using a LINCOplex bead-based array assay (Millipore Corporation, Billerica, MA) on a Bio-Rad Bio-Plex multianalyte detection system (Bio-Rad, Hercules, CA) according to the manufacturers' directions.

Histopathology and Immunohistochemistry

Formalin-fixed pancreatic tumors were embedded in paraffin, cut into 4-μm sections, and processed for either hematoxylin and eosin or immunohistochemical staining at the Histology Core Laboratory at The University of Texas MD Anderson Cancer Center (Smithville, TX). Antibodies used for immunohistochemical analyses were optimized using both positive and negative controls. Slides were deparaffinized and sequentially hydrated in ethanol and water. Antigen retrieval was achieved by microwaving slides for 10 min in 10 mmol/L citrate buffer. Endogenous peroxidase was quenched with 3% hydrogen peroxide for 10 min. Nonspecific binding was inhibited with Biocare blocking reagent (Biocare Medical, Concord, CA) for 30 min at room temperature followed by incubation with primary antibodies (previously described [20]) diluted in blocking buffer. Slides were washed five times with PBS and developed with diaminobenzidine followed by hematoxylin counterstain.

For each immunohistochemical marker, randomly selected slides (eight mice per group) were digitized using the Aperio ScanScope System (ScanScope XT; Aperio Technologies, Vista, CA). Analysis of immunohistochemically stained tumor sections was performed on four fields per slide using the

standard ImageScope membrane/cytoplasmic-specific algorithms to quantify the percentage of cells stained positive for pAkt, pmTOR, pACC, cyclin D1, and cdk4 (cdk4, control, and metformin groups had $n = 7$).

Gene Expression Analysis

RNA was extracted from untreated and treated pancreatic tumor spheres ($n = 3$ per group) and tumor tissue ($n = 6$ per group) using TRI Reagent (Sigma-Aldrich, St. Louis, MO) according to the manufacturer's instructions. Complimentary DNA was synthesized from extracted RNA using the High-Capacity cDNA Reverse Transcription Kit (Applied Biosystems, Foster City, CA) according to the manufacturer's directions. For miR analysis, cDNA was synthesized using TaqMan MicroRNA Reverse Transcription Kit (Applied Biosystems). Gene expression for EMT and miRs was measured by quantitative real-time PCR using TaqMan gene expression assays with TaqMan Universal PCR Master Mix (Applied Biosystems) on an Applied Biosystems ViiA 7 Real-Time PCR System. Expression data for mRNA were normalized to the housekeeping gene, β-actin, whereas miR expression levels were normalized to miR-16 expression. Relative quantitation (RQ) was calculated using the $\Delta\Delta C_t$ method.

Notch1 Luciferase Assay

Luciferase assays were performed to assess whether miR-34a targets the Notch 3′ untranslated region (UTR) in Panc02 cells using LightSwitch 3′ UTR Reporter GoClones, LightSwitch miR mimics, LightSwitch Assay regents, and associated protocols (SwitchGear Genomics, Menlo Park, CA). The experiment was repeated three independent times, and data are presented as mean ± SEM. The mutant Notch1 3′ UTR vector was generated from LightSwitch Notch1 3′ UTR GoClone vector DNA (SwitchGear Genomics) using the QuikChange Lightning Multi Site-Directed Mutagenesis Kit (Agilent Technologies, Santa Clara, CA) according to the manufacturer's instructions. In brief, QuikChange reagents, Notch1 vector (100 ng), and mutagenic primers (Notch 201, 380 ng; Notch 930, 200 ng) were combined and cycled through the thermal cycling program indicated in the manufacturer's protocol. Mutagenic primers were designed to alter the sequence of the Notch1 3′ UTR at the two sites complimentary to the miR-34a seed sequence (target sites) as specified by miRDB, TargetScan, and PicTar. Mutant Notch1 3′ UTR GoClone vector was amplified and selected per the manufacturer's instructions. Plasmids were sequenced at The University of Texas at Austin DNA Core Facility using the following primers: forward, GGGAAGT ACATCAAGAGCTTCGT, and reverse, CCCCCTGAACCT GAAACATAAA.

Tumor Sphere Assay

Panc02 cells were seeded in 96-well low-adherence plates (Corning Inc., Corning, NY) in a serial dilution (from 2,000 to 0 cells per well; six replicates per dilution), as previously described (23). Cells were cultured under serum-free conditions using McCoy's media supplemented with insulin, B27, N2, EGF, and FGF (all from BD Biosciences, San Jose, CA) with/without metformin (0.5 mmol/L) or rapamycin (0.1 mmol/L). Cell media was changed weekly, and tumor spheres were quantified after 14 days. Pancreatic tumor spheres (only those with more than five cells per sphere) were quantified by visual counting at 20× magnification. The diameter of each tumor sphere was measured using SPOT software (Diagnostic Instruments, Sterling Heights, MI). Three independent experiments were performed.

Identification of the $CD24^+CD44^+$ Population in Panc02 Cells

Panc02 cells (~50,000 cells/well) were seeded into six-well plates (Corning Inc.) and left overnight in a 37°C incubator at 5% CO_2. The following day, cells were washed with PBS and then treated with fresh complete McCoy's media in presence or absence of 0.5 mmol/L metformin. After 24–72 h of treatment, cells were washed with PBS, harvested, and stained with anti-mouse antibodies against phycoerythrin-CD24 and allophycocyanin-CD44 (BD Pharmigen) as previously described (23). Each antibody was used at saturating concentrations optimized by initial titrations for flow cytometry staining. The negative control panels were mixtures of isotype controls (eBioscience) diluted to an identical immunoglobulin concentration. Cells were analyzed using Guava Flow Cytometry (Guava Technologies, Hayward, CA), and at least 15,000 events were collected for each sample.

Cell Cycle Analysis

Panc02 cells were treated with complete McCoy's media in the presence or absence of either metformin (0.5 mmol/L) or rapamycin (0.1 mmol/L). Panc02 cells were stained with propidium iodide (PI) according to the manufacturer's instruction (Guava Cell Cycle Reagent; Millipore). Cells serum starved for 24 h were used as a control for G0/G1 phase (quiescent phase). After a 30-min incubation with PI, cells were analyzed using Guava easyCyte Flow Cytometry. Histograms exhibiting G0/G1, S, and G2/M phases were generated using ModFit LT Software (Verity Software House, Topsham, ME). A minimum of three independent experiments were run in which each condition was tested in six replicates.

Statistical Analysis

All statistics were performed using GraphPad Prism 4 (GraphPad Software, San Diego, CA). One-way ANOVA was used to assess differences between vehicle and treatment groups. Two-tailed Student t test was used to assess differences between vehicle control and an individual treatment group. Values of $P < 0.05$ were considered statistically significant.

RESULTS

Body Weight, Caloric Intake, Glucose Tolerance, and Serum Factors

An obese phenotype was attained in all mice prior to drug treatment initiation (15 weeks) as indicated by the increased

mean body weight (40.8 ± 4.7 g) relative to the mean baseline measurement (20.3 ± 29.0 g; $P = 0.0005$) (Fig. 1*A*). After just 4 weeks of treatment, metformin significantly reduced mean body weight relative to vehicle group (41.1 ± 2.7 g vs. 44.8 ± 3.2 g, respectively; $P = 0.0062$), whereas rapamycin treatment did not (46.2 ± 3.5 g) (Fig. 1*A*). Despite these varying effects on body weight, the treatments had no effect on caloric intake (Supplementary Fig. 1). As expected, the metformin group exhibited improved glucose clearance ($P = 0.027$) as well as enhanced insulin sensitivity ($P = 0.038$) relative to vehicle (Fig. 1*B* and *C*). The rapamycin group displayed worsened glucose sensitivity ($P = 0.023$), but it did not affect insulin sensitivity relative to the vehicle group ($P = 0.71$) (Fig. 1*B* and *C*). Fasting levels of circulating insulin were reduced in response to metformin treatment (1.9 ± 0.8 vs. 2.7 ± 0.6 ng/mL; $P = 0.03$) (Fig. 1*D*). Mean circulating levels of the mitogen IGF-1 were nonsignificantly reduced by metformin treatment relative to vehicle (400 ± 35 vs. 420 ± 38 ng/mL; $P = 0.08$) (Fig. 1*E*). No statistical differences were detected between the rapamycin group and the vehicle group regarding insulin (2.6 ± 1.1 ng/mL) or IGF-1 (367 ± 50 ng/mL) levels. Resistin was decreased in the metformin group (2.8 ± 0.4 vs. 3.8 ± 1.5 ng/mL; $P = 0.02$) as well as in the rapamycin group (2.05 ± 0.4 ng/mL) relative to vehicle ($P < 0.001$) (Fig. 1*F*). Serum adiponectin, relative to control, was significantly increased in the metformin group (13.2 ± 1.6 vs. 10.5 ± 2.3 μg/mL; $P = 0.05$) and decreased in the rapamycin group (6.6 ± 0.7 μg/mL; $P < 0.001$) (Fig. 1*G*).

Effect of Metformin on Tumor Growth and Intracellular Signaling Intermediates

At 20 weeks on study, Panc02 cells were injected in the right flank of mice ($n = 15$ per group) that continued on their diet regimen for an additional 4 weeks while tumor growth was monitored. At study termination, tumors were collected form mice. Five mice (control, $n = 4$; metformin, $n = 1$; rapamycin, $n = 1$) were censored from the study due to injection errors. Both metformin (0.62 ± 0.27 g; $P = 0.04$) and rapamycin (0.25 ± 0.33 g; $P < 0.01$) significantly reduced tumor burden compared with vehicle (0.90 ± 0.22 g), although the effect of rapamycin was more dramatic (Fig. 2*A*). Metformin (10.6 ± 3.5%; $P = 0.006$) and rapamycin (19.1 ± 5.7%; $P = 0.05$) both significantly decreased tumoral mTOR activity, assessed by measuring phosphorylation of mTOR, relative to untreated tumors (43.7 ± 8.7%) (Fig. 2*B* and *C*). Despite inhibitory effects on phosphorylation of mTOR, rapamycin treatment (86.3 ± 1.9%; $P = 0.024$), but not metformin treatment (77.2 ± 3.3%), resulted in significantly increased pAkt (Fig. 2*B* and *C*). Metformin (53.7 ± 3.6%; $P = 0.04$) and rapamycin (52.6 ± 3.2%; $P = 0.06$) resulted in a mean increase in phosphorylation of ACC, an inhibitory phosphorylation indicative of AMPK activity as compared with vehicle (37.9 ± 5.6%) (Fig. 2*B* and *C*).

Metformin Increases Expression of miR-34a

Since miRs are aberrantly expressed in many types of cancers, we screened the expression of miRs highly regulated in PC during obesity and diabetes (11) using quantitative real-time PCR (Supplementary Table 1). Validation analysis was performed for those miRs that had *P* values ≤0.15. Validation analysis showed that metformin significantly increased miR-34a expression (RQ = 2.15 ± 1.07 vs. 1.07 ± 0.43; $P = 0.046$) (Fig. 3*A*) and downregulated Notch (RQ = 0.56 ± 0.42 vs. 1.10 ± 0.49; $P = 0.041$) (Fig. 3*B*), an EMT-associated target of miR-34a (24–27), relative to untreated/vehicle controls in both tumors (RQ = 0.61 ± 0.07 vs. 1.5.0 ± 0.15; $P = 0.041$) and in vitro Panc02 cells (RQ = 0.65 ± 0.20 vs. 1.13 ± 0.09 in untreated cells; $P = 0.034$). When Panc02 cells were transfected with Notch reporter plasmid and a miR-34a mimic, luciferase signal was significantly decreased relative to control ($P = 0.007$) (Fig. 3*C*), confirming that Notch is regulated by miR-34a in Panc02 cells. Moreover, after mutating the two miR-34a target sites within the Notch 3′ UTR in the reporter plasmid, no effect of miR-34a on luciferase signal was observed (Fig. 3*D*), indicating that the inhibition of luciferase activity seen in the Notch + miR-34a condition is due to direct binding of miR-34a to Notch in Panc02 cells.

Metformin Decreases Expression of Snail, Vimentin, and Slug in Tumor Samples

Besides Notch, additional EMT markers were found to be regulated by metformin in tumors. As shown in Fig. 4, mRNA expression levels of Snail ($P = 0.049$) and Vimentin ($P = 0.049$) were significantly decreased in the metformin group relative to vehicle. Expression of Slug was also reduced in response to metformin; however, this finding only approached significance ($P = 0.059$).

Rapamycin Increases Expression of Let-7b in Tumors and Inhibits Cell Cycle Progression

Let-7b expression in Panc02 tumors was significantly increased in the rapamycin group relative to vehicle controls (RQ = 1.49 ± 0.22 vs. 1.05 ± 0.37; $P = 0.044$) (Fig. 5*A*). Metformin had no effect on let-7b expression (0.99 ± 0.05; $P = 0.88$) (Fig. 5*A*); however, induction of let-7b expression by metformin has been reported in PC cells (28). Immunohistochemical staining of downstream cell cycle regulatory proteins corroborates this finding by demonstrating that rapamycin significantly reduced expression of cdk4 and cyclin D1 (28.2 ± 3.8%, $P < 0.001$, and 32.0 ± 4.7%, $P = 0.008$, respectively) (Fig. 5*B* and *C*) relative to vehicle (43.5 ± 4.0 and 48.4 ± 3.6%, respectively). Metformin had no significant effect on cyclin D1 (39.4 ± 0.9%) relative to vehicle, although it reduced cdk4 (30.8 ± 4.8%; $P < 0.001$) (Fig. 5*B* and *C*).

Treating Panc02 cells with rapamycin (0.1 mmol/L) significantly increased the percentage of cells arrested in the G0/G1 phase of the cell cycle (50.7 ± 1.7% of positive cells) compared with untreated cells (36.4 ±

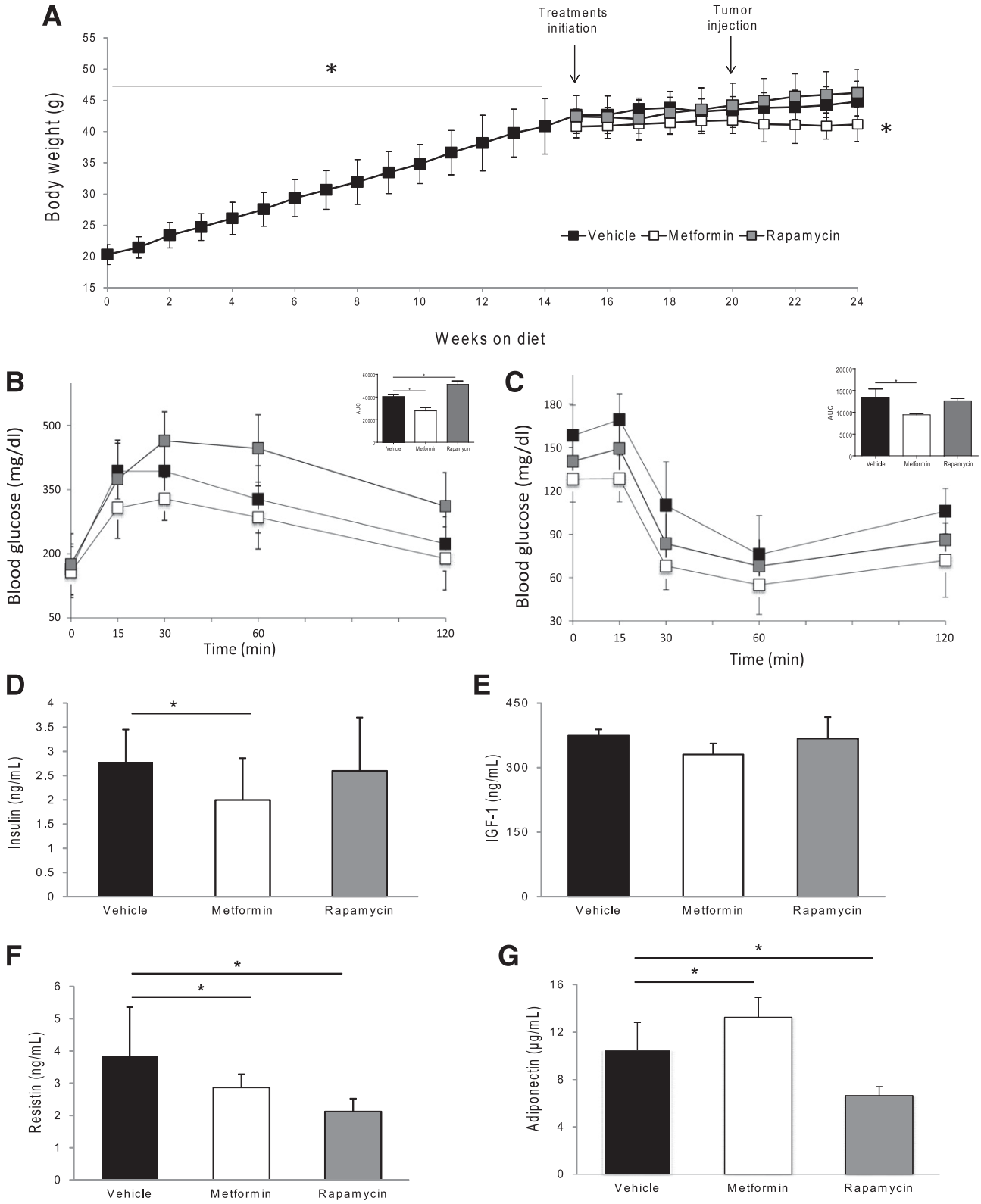

Figure 1—Effect of metformin versus rapamycin on body weight, insulin sensitivity, and serum hormones in obese/prediabetic mice. Treatment conditions (n = 15 per group): vehicle (0.1% DMSO in saline), metformin (250 mg/kg), or rapamycin (2.5 mg/kg). Due to Panc02 cells injection error, 5 mice were censored from the study (vehicle = 11 mice; metformin = 14 mice; rapamycin = 14 mice). *A*: Mean body weight, recorded weekly until study termination. Glucose tolerance test (*B*) and insulin tolerance test (*C*) performed prior to Panc02 cell injection at weeks 19 and 20, respectively (n = 10 per group). Fasting sera harvested at study termination were analyzed for levels of insulin (*D*), IGF-1 (*E*), resistin (*F*), and adiponectin (*G*). The bar graph represents mean ± SD. *$P < 0.05$ by two-tailed Student t test.

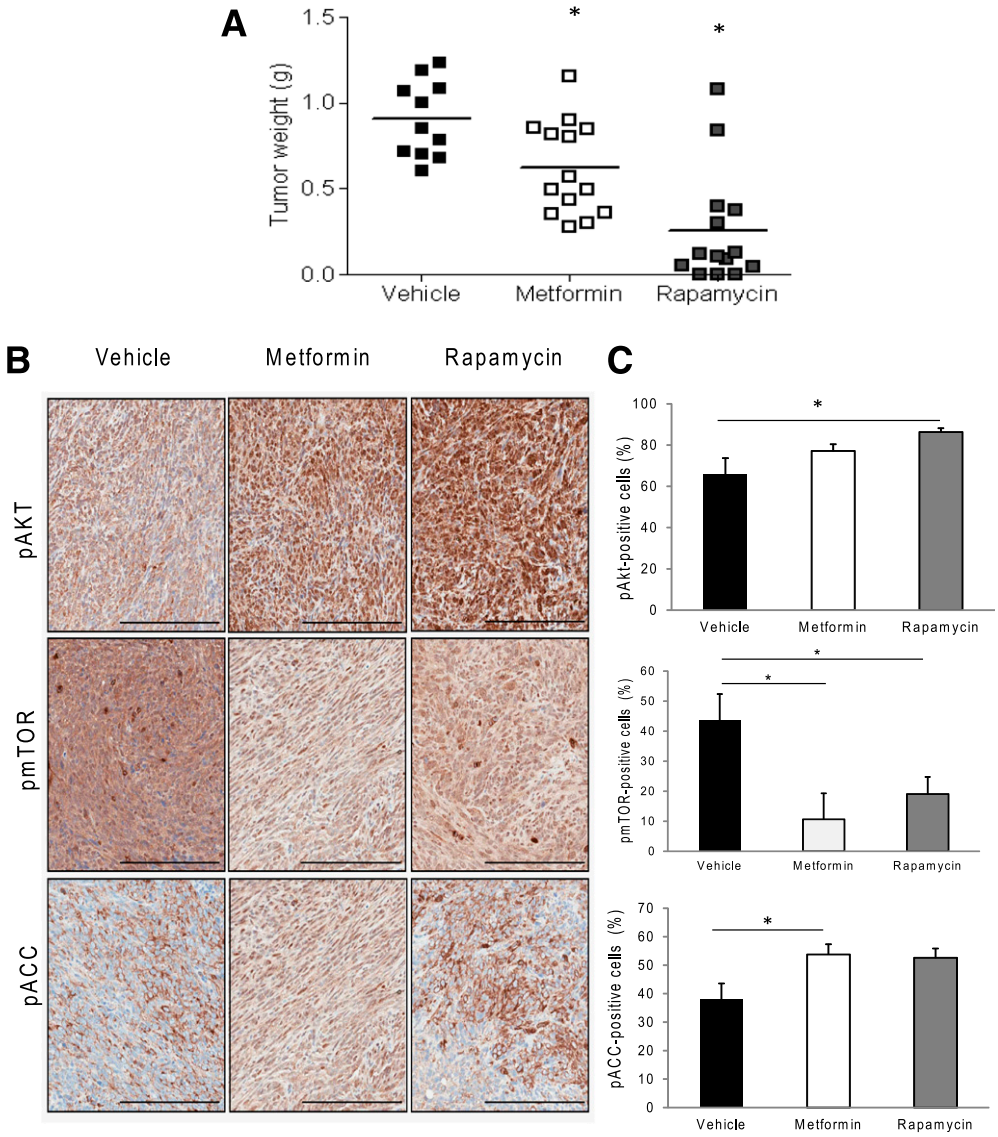

Figure 2—Metformin and rapamycin decreased tumor weights in obese prediabetic mice. *A*: Scatterplot depicting tumor weights measured at study termination in mice receiving either metformin (250 mg/kg, n = 14), rapamycin (2.5 mg/kg, n = 14), or vehicle (0.1% DMSO in saline, n = 11). *B* and *C*: Representative images of pancreatic tumors analyzed by immunohistochemical staining of pAkt, pmTOR, and pACC. *C*: Quantification of pAkt, pmTOR, and pACC positively stained cells in tumor tissues. Original magnification ×40. Scale bar represents 100 nm. Data are expressed as mean ± SEM number of positive cells per field in tumors (n = 8 per group). *P < 0.05 by one-way ANOVA.

1.0%; P = 0.011) (Fig. 5*D* and *E*). Rapamycin also reduced the percentage of cells in S phase (10.5 ± 0.45%) compared with untreated cells (21.3 ± 1.4%; P = 0.048) (Fig. 5*D* and *E*). No major differences were observed in the G2/M phase between treatments. Metformin did not impact cell cycle kinetics relative to untreated cells. Serum-starved Panc02 cells were used as a positive control, causing 70% of total cells to arrest in G0/G1 phase. The decrease in cell cycle progression was not driven by increased apoptosis, since we did not observe any difference in the generation of DNA fragments in rapamycin-treated Panc02 cells compared with untreated cells (Supplementary Fig. 2).

Metformin Reduced Pancreatic Tumor Sphere Formation

Since metformin drastically inhibited pancreatic tumor growth in vivo, we investigated whether this effect was achieved by acting on CSCs, a population with enhanced proliferation and self-renewal properties and characterized by the expression of the cell surface markers CD24 and CD44 (29). We observed that the $CD24^+/CD44^+$ population of Panc02 cells was significantly reduced by metformin compared with untreated controls (63.5 ± 8.5 vs. 76.7 ± 9.4%; P = 0.024) (Fig. 6*A* and *B*). Since tumor sphere–forming capacity has been used to define a more tumorigenic cell population (29), we grew Panc02 cells

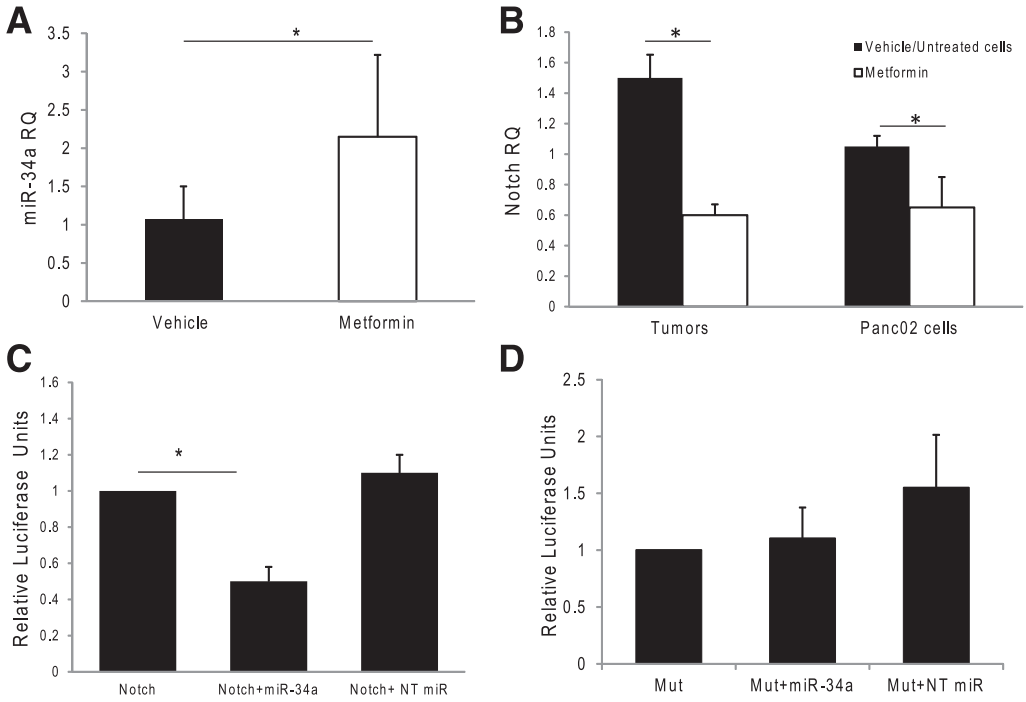

Figure 3—Metformin induced miR-34a expression in pancreatic tumors through direct binding to Notch. *A*: Bar graph of miR-34a expression in pancreatic tumor tissues (n = 6 per group). Data were normalized based on U6 expression. The bar graph represents mean ± SEM. *P < 0.05 by two-tailed Student t test. *B*: Quantification of Notch mRNA expression, relative to β-actin, in tumor samples and Panc02 cells. The bar graph represents mean ± SD. *P < 0.05 by two-tailed Student t test. *C*: Luciferase assay performed on Notch-transfected Pan02 cells in three independent experiments. *D*: Luciferase assay performed on mutated Notch-transfected Pan02 cells in three independent experiments (mutations at two sites in Notch 3′ UTR that are complimentary to the miR-34a seed sequence). The bar graph in *C* and *D* represents mean ± SEM. *P < 0.05 by one-way ANOVA.

into tumor spheres in the presence or absence of metformin and assessed spheroid size and number. After 14 days, metformin (relative to untreated) significantly reduced mean size of Panc02 tumor spheres grown under nonadherent culture conditions by ~50% regardless of initial cell seeding number (from 500 to 2,000 cells) (Fig. 6*C*–*E*). Metformin significantly decreased expression of Notch in tumor spheres (RQ = 0.23 ± 0.006 vs. 1.17 ± 0.64; P = 0.037) compared with untreated tumor spheres (Fig. 6*F*).

DISCUSSION

Our findings establish that both metformin and rapamycin inhibit pancreatic tumor growth in a mouse model of DIO and prediabetes through common and divergent mechanisms. We found that both pharmacologic agents blunted the DIO-associated tumoral activation of mTOR, a crucial complex involved in the regulation of protein translation. Additional data, however, indicate several distinct systemic and intracellular effects of metformin relative to rapamycin, including effects on glucose clearance, circulating levels of energy balance-responsive hormones and growth factors, miR expression, cell cycle regulatory protein expression, and stem cell properties. These findings support epidemiologic data suggesting that metformin, but not other glucose-lowering therapies, may decrease PC risk in the prediabetic and diabetic population as well as minimize PC-related death in patients with diabetes (6–8). They also provide novel insights regarding the shared and distinct mechanisms associated with the anticancer effects of metformin versus the direct mTOR inhibitor rapamycin.

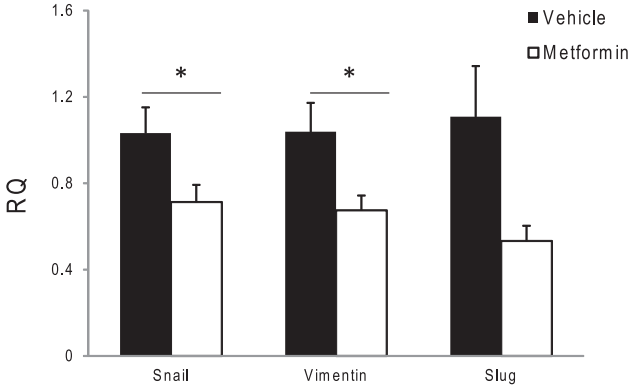

Figure 4—Metformin decreased expression of EMT markers in pancreatic tumors from obese mice. mRNA expression of Snail (P = 0.049), Vimentin (P = 0.049), and Slug (P = 0.059) in tumors treated with metformin (250 mg/kg) and vehicle (0.1% DMSO in saline) (n = 6 per group). The bar graph represents mean ± SEM. *P < 0.05 by Student t test.

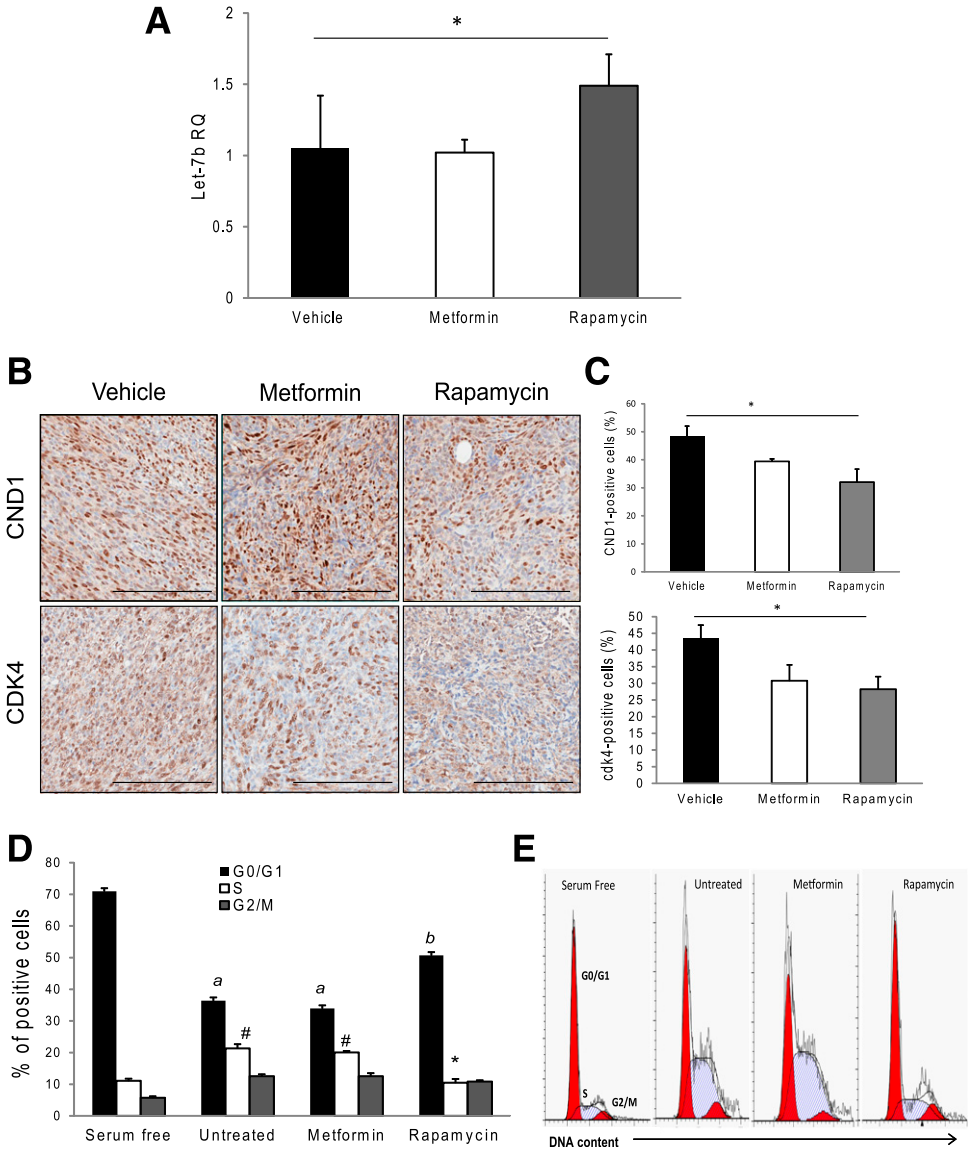

Figure 5—Rapamycin increased let-7b level in pancreatic tumors and inhibited cell cycle progression. *A*: Bar graph representing mean let-7b mRNA expression in tumor tissues (n = 3–6 per group). The bar graph represents mean ± SEM. *P < 0.05 by Student t test. *B* and *C*: Representative images of tumors immunohistochemically stained for the cell cycle regulatory proteins cdk4 and cyclin D1 (*B*) and respective quantification of positively stained cells (n = 8 per group) (*C*). Scale bar represents 100 nm. *D*: Cell cycle analysis (PI staining) of Panc02 cells treated with metformin (0.5 mmol/L) or rapamycin (0.1 mmol/L) for 24 hours (n = 3 per treatment in six replicates). Values within each cell cycle phase with different letters (a,b) or symbols (#,*) are significantly different at P < 0.05. *E*: Histogram representation of the cell cycle phase distribution. The bar graph represents mean ± SEM. *P < 0.05 by one-way ANOVA. The white sphere in *B* (CND1 expression for the rapamycin-treated group) is the cellular outline of a large adipocyte because histological processing with organic solvents extracts the lipid content of cells.

We have previously shown that rapamycin exerts significant tumor growth inhibitory effects in association with diminished mTOR signaling in normoweight mice injected with the same Panc02 tumors used in the present studies (20). In the current report, we show this growth-prohibitive effect of rapamycin in the context of obesity and insulin resistance. Additionally, these findings suggest that a potential mechanism for the inhibitory effects of rapamycin is the increase in let-7b, an miR involved in the regulation of cell proliferation and differentiation, at least in part through regulation of cell cycle regulatory proteins (30–32). In fact, rapamycin treatment resulted in reduced expression of cdk4 and cyclin D1. The composite effect of these outcomes in response to rapamycin treatment was cell cycle inhibition, as evidenced by an accumulation of cells in G0/G1, a finding corroborated by others (33,34).

Specific mTOR inhibition with rapamycin resulted in tumor growth suppression but, unfortunately, was also accompanied by decreased insulin responsiveness and hyperglycemia, consistent with previous reports (35). In contrast, metformin significantly blunted pancreatic tumor growth (albeit to a lesser extent than rapamycin) without

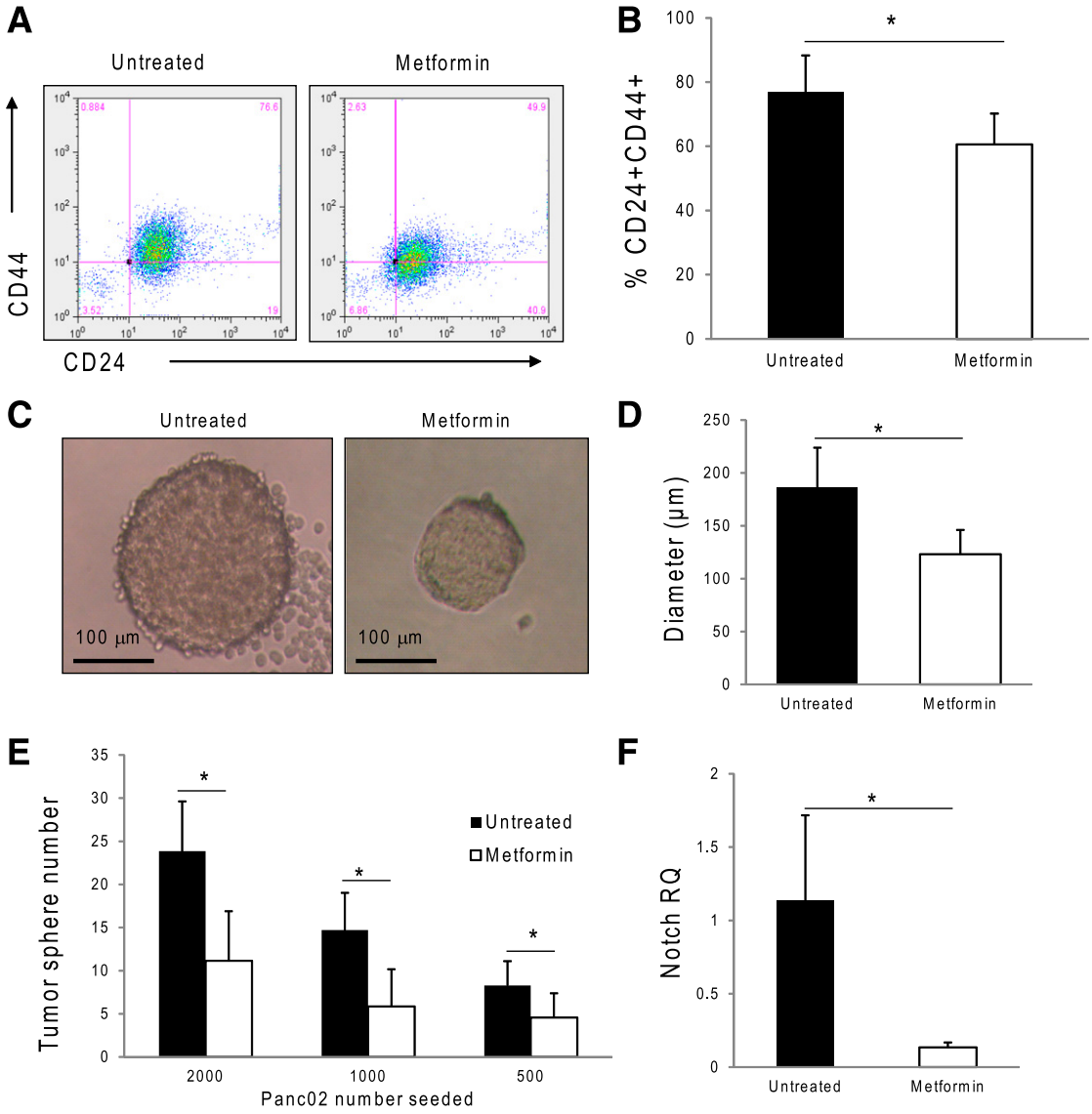

Figure 6—Metformin decreased tumor sphere formation and EMT-associated gene expression in vitro. Distribution (*A*) and quantification (*B*) of the $CD24^+CD44^+$ population in Panc02 cells treated with metformin (0.5 mmol/L) for 24 h ($P = 0.024$). Representative image of Panc02 cells treated with metformin (0.5 mmol/L) for 14 days (*C*), quantification of the mean diameter (*D*), and number of tumor spheres of Panc02 cells treated with metformin (0.5 mmol/L) for 14 days (*E*), relative to untreated control cells. *F*: Bar graph representing Notch mRNA expression in pancreatic tumor spheres treated with metformin (0.5 mmol/L) or control after 14 days of treatment ($n = 3$ per treatment in six replicates). The bar graph represents mean ± SD. *$P < 0.05$ by Student *t* test.

apparent adverse metabolic effects, similar to previous observations (36). In our study, we found that metformin resulted in improved glucose and insulin metabolism and a serum profile (decreased IGF-1, insulin, and resistin; increased adiponectin) associated with normalization of metabolic state and tumor growth inhibition in DIO mice (20,37,38). Similar to previous reports (39), we found that metformin induced tumoral expression of miR-34a, an miR typically lost during cancer progression, including pancreatic (24,40), and has been shown to contribute to reduced survivability in those diagnosed with PC (41). miR-34a suppresses EMT by acting as a negative regulator of the signaling pathway activated by transforming growth factor-β (TGF-β), a master regulator of EMT (42). Interestingly, metformin has been shown to inhibit TGF-β–induced EMT in breast cancer cells, particularly stem cell–enriched populations, as well as alter expression of EMT mediators (43). Expression of these mediators, such as Snail, is intimately linked to TGF-β signaling and miR-34a expression. Specifically, as TGF-β increases, expression of miR-34a is diminished and Snail is enhanced (42), whereas re-expression of miR-34a reduces expression of Snail and other EMT mediators such as Notch and Slug (44). Our in vitro results corroborated these findings by demonstrating that targeted binding of miR-34a regulated expression of Notch in Panc02 cells, further suggesting that metformin may modulate EMT-related targets, such as Notch, in a miR-34a–dependent manner in Panc02 tumors. Panc02 tumor

spheres also had reduced Notch expression in response to metformin. Dysregulation of Notch signaling, a targeted perturbation in many cancer types (24,45), has been shown to enhance hypoxia-induced tumor cell migration and invasion and influence expression of Snail and Slug (46,47). Additionally, metformin reduced the $CD24^+/CD44^+$ cell population and decreased the tumor sphere–forming capacity of Panc02 cells, corroborating previous findings that metformin significantly reduced CSC enrichment in pancreatic tumors (28). The importance of this TGF-β/miR-34a pathway cannot be understated in the context of Panc02 cells, which have a mutation in Smad4 (a downstream regulator of TGF-β signaling), a genetic anomaly that is found in ~55% of all pancreatic ductal adenocarcinomas and is predictive of poor prognosis (48). Loss of Smad functioning can alter miR expression profiles (49), but metformin, in our study, overcame the loss of miR-34a. This suggests that metformin may be able to blunt the protumorigenic nature of genetic alterations such as Smad4 mutation, possibly in part through negatively regulating the EMT.

In summary, these preclinical findings suggest metformin and rapamycin can both inhibit diabetes-associated pancreatic tumor growth through common and distinct miR-mediated mechanisms. We conclude that metformin and direct mTOR inhibitors, alone or possibly in combination, represent promising interventions that should be tested in future translational studies evaluating new strategies for breaking the diabetes-PC link.

Funding. This study was supported by grant R01-CA-135386 (S.D.H.).

Duality of Interest. No potential conflicts of interest relevant to this article were reported.

Author Contributions. V.C. performed the majority of in vitro and animal studies, analyzed and interpreted the data, and wrote and critically revised the manuscript. L.M.L. helped perform the animal studies, analyzed and interpreted the data, and critically revised the manuscript. K.L.D. performed miR experiments and critically revised the article. S.M.D. conceptualized and assisted with the in vitro experiments. J.H. analyzed and interpreted immunohistochemical images and critically revised the manuscript. R.K. and M.N.P. conceptualized the study and critically revised the manuscript. S.D.H. conceptualized the study, coordinated the research team, interpreted the data, and revised the manuscript. S.D.H. is the guarantor of this work and, as such, had full access to all the data in the study and takes responsibility for the integrity of the data and the accuracy of the data analysis.

References

1. Campbell PT, Newton CC, Patel AV, Jacobs EJ, Gapstur SM. Diabetes and cause-specific mortality in a prospective cohort of one million U.S. adults. Diabetes Care 2012;35:1835–1844

2. Everhart J, Wright D. Diabetes mellitus as a risk factor for pancreatic cancer. A meta-analysis. JAMA 1995;273:1605–1609

3. Huxley R, Ansary-Moghaddam A, Berrington de González A, Barzi F, Woodward M. Type-II diabetes and pancreatic cancer: a meta-analysis of 36 studies. Br J Cancer 2005;92:2076–2083

4. Wang F, Herrington M, Larsson J, Permert J. The relationship between diabetes and pancreatic cancer. Mol Cancer 2003;2:4

5. Wiernsperger NF, Bailey CJ. The antihyperglycaemic effect of metformin: therapeutic and cellular mechanisms. Drugs 1999;58(Suppl. 1):31–39; discussion 75–82

6. Currie CJ, Poole CD, Gale EA. The influence of glucose-lowering therapies on cancer risk in type 2 diabetes. Diabetologia 2009;52:1766–1777

7. Evans JM, Donnelly LA, Emslie-Smith AM, Alessi DR, Morris AD. Metformin and reduced risk of cancer in diabetic patients. BMJ 2005;330:1304–1305

8. Sadeghi N, Abbruzzese JL, Yeung SC, Hassan M, Li D. Metformin use is associated with better survival of diabetic patients with pancreatic cancer. Clin Cancer Res 2012;18:2905–2912

9. Singh S, Singh PP, Singh AG, Murad MH, McWilliams RR, Chari ST. Anti-diabetic medications and risk of pancreatic cancer in patients with diabetes mellitus: a systematic review and meta-analysis. Am J Gastroenterol 2013;108:510–519; quiz 520

10. Suissa S, Azoulay L. Metformin and the risk of cancer: time-related biases in observational studies. Diabetes Care 2012;35:2665–2673

11. Bao B, Wang Z, Li Y, Kong D, Ali S, Banerjee S, Ahmad A, Sarkar FH. The complexities of obesity and diabetes with the development and progression of pancreatic cancer. Biochim Biophys Acta 2011;1815:135–146

12. Nair V, Sreevalsan S, Basha R, et al. Mechanism of metformin-dependent inhibition of mammalian target of rapamycin (mTOR) and Ras activity in pancreatic cancer: role of specificity protein (Sp) transcription factors. J Biol Chem 2014;289:27692–27701

13. Hardie DG, Ross FA, Hawley SA. AMPK: a nutrient and energy sensor that maintains energy homeostasis. Nat Rev Mol Cell Biol 2012;13:251–262

14. Wullschleger S, Loewith R, Oppliger W, Hall MN. Molecular organization of target of rapamycin complex 2. J Biol Chem 2005;280:30697–30704

15. Alimova IN, Liu B, Fan Z, et al. Metformin inhibits breast cancer cell growth, colony formation and induces cell cycle arrest in vitro. Cell Cycle 2009;8:909–915

16. Bruns CJ, Koehl GE, Guba M, et al. Rapamycin-induced endothelial cell death and tumor vessel thrombosis potentiate cytotoxic therapy against pancreatic cancer. Clin Cancer Res 2004;10:2109–2119

17. Stephan S, Datta K, Wang E, et al. Effect of rapamycin alone and in combination with antiangiogenesis therapy in an orthotopic model of human pancreatic cancer. Clin Cancer Res 2004;10:6993–7000

18. Bartel DP. MicroRNAs: genomics, biogenesis, mechanism, and function. Cell 2004;116:281–297

19. Gregory PA, Bracken CP, Bert AG, Goodall GJ. MicroRNAs as regulators of epithelial-mesenchymal transition. Cell Cycle 2008;7:3112–3118

20. Lashinger LM, Malone LM, Brown GW, et al. Rapamycin partially mimics the anticancer effects of calorie restriction in a murine model of pancreatic cancer. Cancer Prev Res (Phila) 2011;4:1041–1051

21. Brüning JC, Winnay J, Bonner-Weir S, Taylor SI, Accili D, Kahn CR. Development of a novel polygenic model of NIDDM in mice heterozygous for IR and IRS-1 null alleles. Cell 1997;88:561–572

22. Corbett TH, Roberts BJ, Leopold WR, et al. Induction and chemotherapeutic response of two transplantable ductal adenocarcinomas of the pancreas in C57BL/6 mice. Cancer Res 1984;44:717–726

23. Dunlap SM, Chiao LJ, Nogueira L, et al. Dietary energy balance modulates epithelial-to-mesenchymal transition and tumor progression in murine claudin-low and basal-like mammary tumor models. Cancer Prev Res (Phila) 2012;5:930–942

24. Kashat M, Azzouz L, Sarkar SH, Kong D, Li Y, Sarkar FH. Inactivation of AR and Notch-1 signaling by miR-34a attenuates prostate cancer aggressiveness. Am J Transl Res 2012;4:432–442

25. Ye QF, Zhang YC, Peng XQ, Long Z, Ming YZ, He LY. siRNA-mediated silencing of Notch-1 enhances docetaxel induced mitotic arrest and apoptosis in prostate cancer cells. Asian Pac J Cancer Prev 2012;13:2485–2489

26. Ye QF, Zhang YC, Peng XQ, Long Z, Ming YZ, He LY. Silencing Notch-1 induces apoptosis and increases the chemosensitivity of prostate cancer cells to docetaxel through Bcl-2 and Bax. Oncol Lett 2012;3:879–884

27. Yu Z, Pestell TG, Lisanti MP, Pestell RG. Cancer stem cells. Int J Biochem Cell Biol 2012;44:2144–2151

28. Bao B, Wang Z, Ali S, et al. Metformin inhibits cell proliferation, migration and invasion by attenuating CSC function mediated by deregulating miRNAs in pancreatic cancer cells. Cancer Prev Res (Phila) 2012;5:355–364
29. Mani SA, Guo W, Liao MJ, et al. The epithelial-mesenchymal transition generates cells with properties of stem cells. Cell 2008;133:704–715
30. Boyerinas B, Park SM, Hau A, Murmann AE, Peter ME. The role of let-7 in cell differentiation and cancer. Endocr Relat Cancer 2010;17:F19–F36
31. Johnson SM, Grosshans H, Shingara J, et al. RAS is regulated by the let-7 microRNA family. Cell 2005;120:635–647
32. Miska EA, Alvarez-Saavedra E, Townsend M, et al. Microarray analysis of microRNA expression in the developing mammalian brain. Genome Biol 2004;5: R68
33. Decker T, Hipp S, Ringshausen I, et al. Rapamycin-induced G1 arrest in cycling B-CLL cells is associated with reduced expression of cyclin D3, cyclin E, cyclin A, and survivin. Blood 2003;101:278–285
34. Noh WC, Mondesire WH, Peng J, et al. Determinants of rapamycin sensitivity in breast cancer cells. Clin Cancer Res 2004;10:1013–1023
35. Lamming DW, Ye L, Katajisto P, et al. Rapamycin-induced insulin resistance is mediated by mTORC2 loss and uncoupled from longevity. Science 2012;335: 1638–1643
36. Schneider MB, Matsuzaki H, Haorah J, et al. Prevention of pancreatic cancer induction in hamsters by metformin. Gastroenterology 2001;120:1263–1270
37. Nunez NP, Perkins SN, Smith NC, et al. Obesity accelerates mouse mammary tumor growth in the absence of ovarian hormones. Nutr Cancer 2008;60: 534–541
38. Lashinger LM, Harrison LM, Rasmussen AJ, et al. Dietary energy balance modulation of Kras- and Ink4a/Arf+/–driven pancreatic cancer: the role of insulin-like growth factor-I. Cancer Prev Res (Phila) 2013;6:1046–1055
39. Do MT, Kim HG, Choi JH, Jeong HG. Metformin induces microRNA-34a to downregulate the Sirt1/Pgc-1α/Nrf2 pathway, leading to increased susceptibility of wild-type p53 cancer cells to oxidative stress and therapeutic agents. Free Radic Biol Med 2014;74:21–34
40. Ji Q, Hao X, Zhang M, et al. MicroRNA miR-34 inhibits human pancreatic cancer tumor-initiating cells. PLoS ONE 2009;4:e6816
41. Jamieson NB, Morran DC, Morton JP, et al. MicroRNA molecular profiles associated with diagnosis, clinicopathologic criteria, and overall survival in patients with resectable pancreatic ductal adenocarcinoma. Clin Cancer Res 2012; 18:534–545
42. Zhang J, Tian XJ, Zhang H, et al. TGF-β-induced epithelial-to-mesenchymal transition proceeds through stepwise activation of multiple feedback loops. Sci Signal 2014;7:ra91
43. Cufí S, Vazquez-Martin A, Oliveras-Ferraros C, Martin-Castillo B, Joven J, Menendez JA. Metformin against TGFβ-induced epithelial-to-mesenchymal transition (EMT): from cancer stem cells to aging-associated fibrosis. Cell Cycle 2010;9:4461–4468
44. Niessen K, Fu Y, Chang L, Hoodless PA, McFadden D, Karsan A. Slug is a direct Notch target required for initiation of cardiac cushion cellularization. J Cell Biol 2008;182:315–325
45. Wang Z, Li Y, Banerjee S, Sarkar FH. Emerging role of Notch in stem cells and cancer. Cancer Lett 2009;279:8–12
46. Leong KG, Niessen K, Kulic I, et al. Jagged1-mediated Notch activation induces epithelial-to-mesenchymal transition through Slug-induced repression of E-cadherin. J Exp Med 2007;204:2935–2948
47. Sahlgren C, Gustafsson MV, Jin S, Poellinger L, Lendahl U. Notch signaling mediates hypoxia-induced tumor cell migration and invasion. Proc Natl Acad Sci U S A 2008;105:6392–6397
48. Wang Y, Zhang Y, Yang J, et al. Genomic sequencing of key genes in mouse pancreatic cancer cells. Curr Mol Med 2012;12:331–341
49. Li L, Li Z, Kong X, et al. Down-regulation of microRNA-494 via loss of SMAD4 increases FOXM1 and beta-catenin signaling in pancreatic ductal adenocarcinoma cells. Gastroenterology 2014;147:485–497.e18